THE ASTRONOMICAL JOURNAL, 122:2850–2857, 2001 December

EVIDENCE FOR REIONIZATION AT $z \sim 6$: DETECTION OF A GUNN-PETERSON TROUGH IN A $z = 6.28$ QUASAR[1,2]

ROBERT H. BECKER,[3,4] XIAOHUI FAN,[5] RICHARD L. WHITE,[6] MICHAEL A. STRAUSS,[7] VIJAY K. NARAYANAN,[7] ROBERT H. LUPTON,[7] JAMES E. GUNN,[7] JAMES ANNIS,[8] NETA A. BAHCALL,[7] J. BRINKMANN,[9] A. J. CONNOLLY,[10] ISTVÁN CSABAI,[11,12] PAUL C. CZARAPATA,[8] MAMORU DOI,[13] TIMOTHY M. HECKMAN,[11] G. S. HENNESSY,[14] ŽELJKO IVEZIĆ,[7] G. R. KNAPP,[7] DON Q. LAMB,[15] TIMOTHY A. MCKAY,[16] JEFFREY A. MUNN,[17] THOMAS NASH,[8] ROBERT NICHOL,[18] JEFFREY R. PIER,[17] GORDON T. RICHARDS,[19] DONALD P. SCHNEIDER,[19] CHRIS STOUGHTON,[8] ALEXANDER S. SZALAY,[11] ANIRUDDHA R. THAKAR,[11] AND D. G. YORK[15,20]

Received 2001 August 6; accepted 2001 September 4

ABSTRACT

We present moderate-resolution Keck spectroscopy of quasars at $z = 5.82$, 5.99, and 6.28, discovered by the Sloan Digital Sky Survey (SDSS). We find that the Lyα absorption in the spectra of these quasars evolves strongly with redshift. To $z \sim 5.7$, the Lyα absorption evolves as expected from an extrapolation from lower redshifts. However, in the highest-redshift object, SDSSp J103027.10+052455.0 ($z = 6.28$), the average transmitted flux is 0.0038 ± 0.0026 times that of the continuum level over 8450 Å $< \lambda <$ 8710 Å ($5.95 < z_{\rm abs} < 6.16$), consistent with zero flux. Thus the flux level drops by a factor of greater than 150 and is consistent with zero flux in the Lyα forest region immediately blueward of the Lyα emission line, compared with a drop by a factor of $\sim$10 at $z_{\rm abs} \sim 5.3$. A similar break is seen at Lyβ; because of the decreased oscillator strength of this transition, this allows us to put a considerably stronger limit, $\tau_{\rm eff} > 20$, on the optical depth to Lyα absorption at $z = 6$. This is a clear detection of a complete Gunn-Peterson trough, caused by neutral hydrogen in the intergalactic medium. Even a small neutral hydrogen fraction in the intergalactic medium would result in an undetectable flux in the Lyα forest region. Therefore, the existence of the Gunn-Peterson trough by itself does not indicate that the quasar is observed prior to the reionization epoch. However, the fast evolution of the mean absorption in these high-redshift quasars suggests that the mean ionizing background along the line of sight to this quasar has declined significantly from $z \sim 5$ to 6, and the universe is approaching the reionization epoch at $z \sim 6$.

Key words: cosmology: observations — galaxies: formation — quasars: absorption lines — quasars: general

1. INTRODUCTION

Recent discoveries of quasars at redshifts of 5.8 and greater (Fan et al. 2000, 2001a, hereafter Paper I) are finally allowing quantitative studies of the status of the intergalactic medium (IGM) and the history of reionization at redshifts near 6. The absence of a Gunn-Peterson trough (Shklovsky 1964; Scheuer 1965; Gunn & Peterson 1965) in the spectrum of the $z = 5.8$ quasar SDSSp J104433.4−012502.2 (SDSS 1044−0125 for brevity, Fan et al. 2000; see Goodrich et al. 2001 for an updated redshift based on the C IV line in the near-infrared) indicates that the IGM is already highly ionized at $z \sim 5.5$, presumably by the UV-ionizing photons from quasars and star-forming galaxies at high redshift. In Paper I, we used the low-resolution

[1] Based on observations obtained at the W. M. Keck Observatory, which is operated as a scientific partnership among the California Institute of Technology, the University of California and the National Aeronautics and Space Administration, made possible by the generous financial support of the W. M. Keck Foundation, and with the Sloan Digital Sky Survey, which is owned and operated by the Astrophysical Research Consortium.

[2] This paper is dedicated to the memory of Arthur F. Davidsen (1944–2001), a pioneer in the study of the intergalactic medium and a leader in the development of the Sloan Digital Sky Survey.

[3] Department of Physics, University of California at Davis, Davis, CA 95616.
[4] IGPP/Lawrence Livermore National Laboratory, Livermore, CA 94550.
[5] Institute for Advanced Study, Olden Lane, Princeton, NJ 08540.
[6] Space Telescope Science Institute, 3700 San Martin Drive, Baltimore, MD 21218.
[7] Princeton University Observatory, Princeton, NJ 08544.
[8] Fermi National Accelerator Laboratory, P.O. Box 500, Batavia, IL 60510.
[9] Apache Point Observatory, P.O. Box 49, Sunspot, NM 88349.
[10] Department of Physics and Astronomy, University of Pittsburgh, Pittsburgh, PA 15260.
[11] Department of Physics and Astronomy, Johns Hopkins University, 3400 North Charles Street, Baltimore, MD 21218.
[12] Department of Physics of Complex Systems, Eötvös University, H-1117 Budapest, Hungary.
[13] Department of Astronomy and Research Center for the Early Universe, School of Science, University of Tokyo, Hongo, Bunkyo, Tokyo 113-0033, Japan.
[14] US Naval Observatory, 3450 Massachusetts Avenue, NW, Washington, DC 20392-5420.
[15] Astronomy and Astrophysics Center, University of Chicago, 5640 South Ellis Avenue, Chicago, IL 60637.
[16] Department of Physics, University of Michigan, 500 East University, Ann Arbor, MI 48109.
[17] US Naval Observatory, Flagstaff Station, P.O. Box 1149, Flagstaff, AZ 86002-1149.
[18] Department of Physics, Carnegie Mellon University, 5000 Forbes Avenue, Pittsburgh, PA 15232.
[19] Department of Astronomy and Astrophysics, Pennsylvania State University, University Park, PA 16802.
[20] Enrico Fermi Institute, 5640 South Ellis Avenue, Chicago, IL 60637.

discovery spectra of the three new quasars at $z > 5.8$, taken with the ARC 3.5 m telescope at Apache Point Observatory, to show that Lyα absorption increases significantly from a redshift of 5.5 to a redshift of 6.0. In particular, the spectrum of the $z = 6.28$ quasar SDSSp J103027.10+052455.0 shows that in a $\sim$300 Å region of the Lyα forest immediately blueward of the Lyα emission line, the flux level is consistent with zero, indicating a flux decrement of $\gtrsim$50 and suggesting a possible detection of the complete Gunn-Peterson trough. To more accurately quantify this effect and to constrain the properties of the IGM, we have obtained higher resolution spectra of the three new $z > 5.8$ quasars using the Echelle Spectrograph and Imager (ESI; Epps & Miller 1998) on the Keck II telescope.

In § 2 we describe the observations and present the spectra of all four $z \gtrsim 5.8$ quasars in the sample of Fan et al. (2001a). We measure the emission-line redshifts of the three new quasars using these spectra. In § 3, we discuss the properties of the Lyα forest in the four spectra from the point of view of the overall opacity of the IGM as a function of redshift. In § 4 we discuss the cosmological implications of the results.

2. SPECTROSCOPIC OBSERVATIONS

SDSSp J083643.85+005453.3 ($z = 5.82$), SDSSp J130608.26+035626.3 ($z = 5.99$), and SDSSp J103027.10+052455.0 ($z = 6.28$) (referred to as SDSS 0836+0054, SDSS 1306+0356, and SDSS 1030+0524 throughout this paper for brevity) were selected as *i*-dropout objects from the Sloan Digital Sky Survey (SDSS, York et al. 2000) multicolor imaging data. They were further separated from cool dwarfs using follow-up *J*-band photometry, and discovery spectra were obtained using the Double Imaging Spectrograph (DIS), a low-resolution spectrograph ($R \sim 500$) on the ARC 3.5 m telescope at the Apache Point Observatory (Paper I).

In 2001 March and May, we obtained moderate-resolution spectra of these three high-redshift quasars, using ESI on the Keck II telescope. The spectra were taken in the echellette mode of ESI. In this mode, the spectral range from 4000 to 10,000 Å is covered in 10 spectral orders with a constant dispersion of 11.4 km s^{-1} pixel^{-1}. With a plate scale ranging from 0.″142 to 0.″128 pixel^{-1} in the three reddest orders, the 1″ slit has a footprint of 81–90 km s^{-1} and the $\sim$0.″7 typical seeing has a footprint of 57–63 km s^{-1}. Using the skylines in the spectrum, we estimate that the FWHM of the instrument profile is $\sim$1.8 Å at $\sim$8500 Å, indicating a spectral resolution of 66 km s^{-1}, or $R \sim 4700$, almost 10 times higher than that of the discovery spectra. Wavelength calibration is based on observations of Hg-Ne-Xe lamps and Cu-Ar lamps. The ESI has active flexure control that minimizes any drift in the wavelength calibration or fringing pattern. This is especially important for accurate sky subtraction—a crucial step in detecting the faint flux in the quasar Lyα forest region in the presence of strong sky emission lines. The spectrophotometric standard G191-B2B (Massey 1988; Massey & Gronwall 1990) was observed for flux calibration. The standard star, observed at similar air mass as the quasars, was also used for tracing the spectra in the spectral region where little flux is detected from the quasar because of strong Lyα absorption. All the observations were made at the parallactic angle. Data reduction made use of standard IRAF routines along with a suite of custom analysis routines that handle the large curvature, highly nonlinear photometric response, and slight tilt of the skylines in the ESI instrument. The dates and durations of the exposures are given in Table 1.

The three spectra are displayed in Figure 1, along with the spectrum of SDSS 1044−0125, which was observed an year earlier with the same instrument setting (Fig. 2 of Fan et al. 2000). The spectra are binned to 4 Å pixel^{-1} to improve the signal-to-noise ratio (S/N), and the flux levels are adjusted to match the *z*-band photometry presented in Paper I. Each pixel is weighted by the inverse square of the estimated noise on that pixel when the high-resolution spectrum is binned to low resolution. It is clear from a visual inspection of the four spectra that the flux level blueward of Lyα decreases with increasing redshift and is consistent with zero flux in SDSS 1030+0524.

Using these spectra, we first determine accurate redshifts from the emission lines. As discussed in Fan et al. (2000) and in Paper I, redshift determination of $z > 5.5$ quasars using optical spectra is difficult, because of the weakness of the accessible metal emission lines and the effect of Lyα forest absorption on the Lyα emission line. The presence of associated metal absorption lines would also bias the result (Goodrich et al. 2001). The strong C IV emission line, now at $\lambda > 10{,}000$ Å, would provide a more reliable redshift measurement, but it lies beyond our spectral coverage for all our objects.

SDSS 1044−0125: As mentioned above, the displayed spectrum is from Fan et al. (2000). Djorgovski et al. (2001) present a higher S/N spectrum of SDSS 1044−0125, which shows the increasing optical depth of the Lyα forest with redshift particularly well.

SDSS 0836+0054: A strong O I + Si II λ1302 emission line is detected at $\lambda = 8873 \pm 1$ Å, with a rest-frame equivalent width (EW) of 4.2 ± 0.1 Å. The Lyα + N V emission line is very broad, with the peak wavelength of the Lyα component at $\sim$8230 Å and EW = 70 ± 3 Å. We adopt a redshift of 5.82, using the central wavelength of O I line and a redshift error of 0.02, considering the uncertainty using a single line for redshift. The peak of the Lyα emission line is consistent with this redshift. The EW of O I + Si II is comparable to that of the average of $z \sim 4$ quasars (3.2 Å, Schneider, Schmidt, & Gunn 1991).

SDSS 1306+0356: The strong Lyα + N V emission line shows a separate N V λ1240 component. We determine the central wavelengths and EWs of Lyα and N V by fitting two Gaussian profiles to the wavelength range redward of the peak of Lyα emission, i.e., the region not affected by the Lyα forest absorption. The wavelength ratio of the two components is fixed in the fitting procedure. We find $z_{em} = 5.99$, EW(Lyα) = 38.1 ± 14.9 Å, and EW(N V) = 17.9 ± 6.3 Å. No obvious O I + Si II emission line is detected; any emission line there is probably affected by the C IV absorption feature at the same wavelength (see below). A possible Si IV

TABLE 1

OBSERVING LOG

Object	Redshift (z_{em})	Date	Exposure Time (s)
J104433.04–012502.2.....	5.80	2000 Mar 04	2 × 1200
J083643.85+005453.3.....	5.82	2001 Mar 19	1200
J130608.26+035626.3.....	5.99	2001 May 26	900
J103027.10+052455.0.....	6.28	2001 May 26	2 × 900

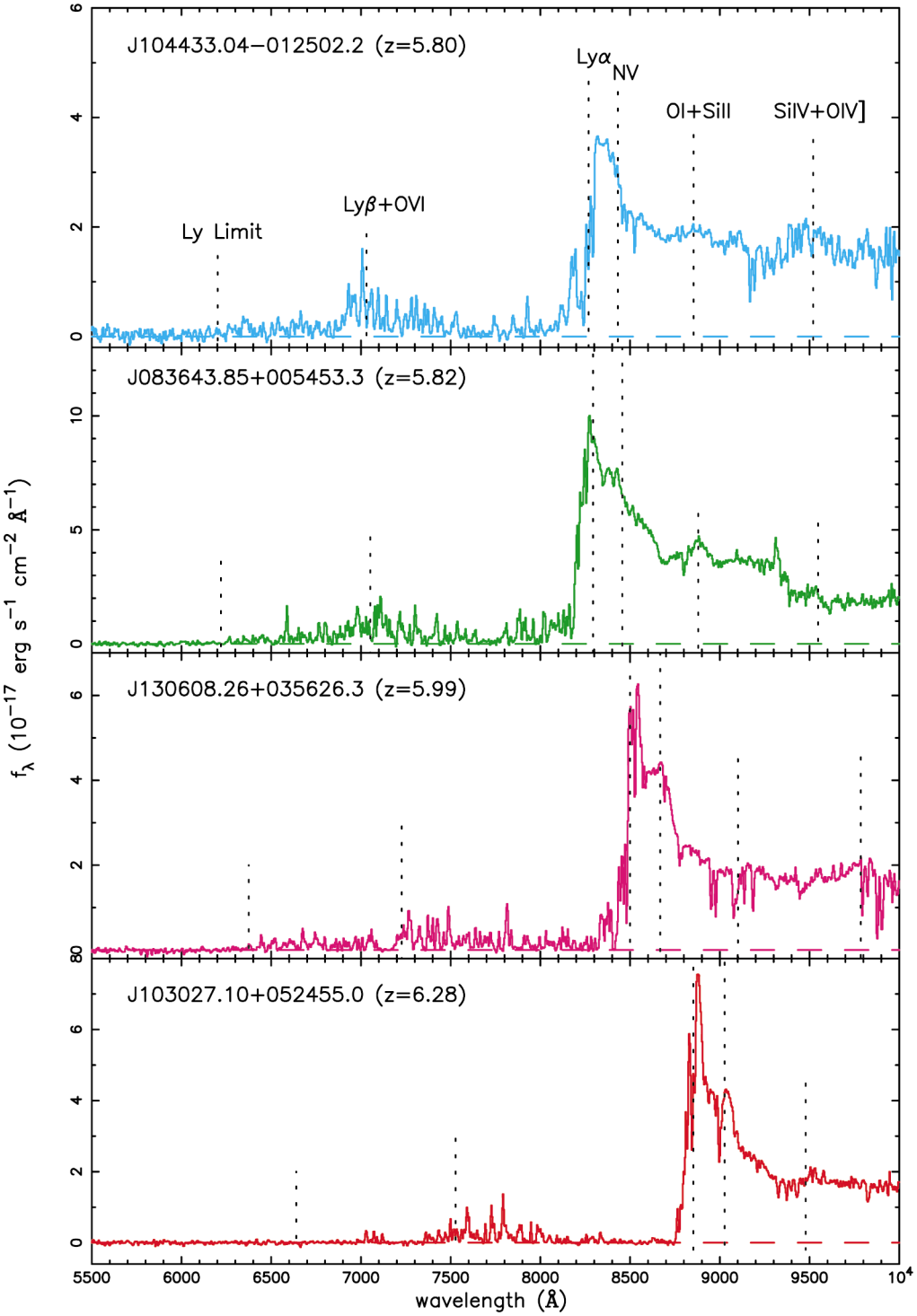

FIG. 1.—Optical spectra of $z \gtrsim 5.8$ quasars observed with Keck/ESI in the observed frame. The spectra have been smoothed to 4 Å pixel^{-1} and have been normalized to the observed z-band flux. The spectrum of SDSS 1044−0125 has been taken from Fan et al. (2000). In each spectrum, the expected wavelengths of prominent emission lines, as well as the Lyman limit, are indicated by the dashed lines.

λ1402 feature is detected at $\sim$9800 Å, but it is difficult to fit its profile because of the weakness of the line and possible absorption lines nearby. We therefore adopt a redshift of 5.99 ± 0.02 for SDSS 1306+0356.

In the spectrum of SDSS 1306+0356, we notice a strong absorption feature at $\sim$7130 Å, where over $\sim$80 Å there is no detectable flux. The rest-frame equivalent width is $\sim$15 Å, typical for a damped Lyα system, at a redshift of $z_{\rm abs} =$ 4.86. A strong absorption feature is detected at $\lambda = 9080$ Å, corresponding to C IV absorption at the same redshift. This feature is double peaked in absorption, consistent with the $\lambda\lambda$1548, 1551 components of the C IV doublet, although the signal-to-noise ratio is low at that wavelength. This system, if confirmed by high-S/N spectroscopy, is the highest-redshift damped Lyα system known (the previous record holder was at $z = 4.47$, Péroux et al. 2001; Dessauges-

Zavadsky et al. 2001). The two other doublet absorption features at $\sim$9900 and $\sim$8960 Å are identified as Mg II absorptions at $z = 2.53$ and 2.20, respectively. Note that other spectra in this paper also show various absorption features redward of Lyα emission. The detailed identifications of these metal lines are beyond the scope of this paper.

SDSS 1030+0524: In Paper I we presented the Keck NIRSPEC J-band spectrum of this object, in which a strong C IV feature (EW = 31.5 ± 8.6Å) is detected at $z = 6.28 \pm 0.02$. The optical spectrum shows a separate N V emission line and possible detection of O I + Si II and Si IV lines at the same redshift. We measure EW(Lyα) = 40.9 ± 7.4 Å and EW(N V) = 16.9 ± 4.0 Å by fitting Gaussian profiles to the blended Lyα + N V emission line.

Paper I discusses the implication of the detection of metal emission lines, in particular that of N V emission, for the metallicity of the quasar environment. Assuming a power-law continuum of $f_\nu \propto \nu^{-0.5}$, the flux ratio N V/C IV is 0.74 ± 0.27, consistent with a supersolar metallicity $Z \gtrsim 3\ Z_\odot$ according to the calculations of Hamann & Ferland (1993). Note, however, these calculations assume a single-zone photoionization model and might be affected by the uncertainties in heavy element ratios, as well as possible enhancement of N V flux by resonant scattering from the red wing of the Lyα emission line (Krolik & Voit 1998).

3. NEUTRAL HYDROGEN ABSORPTION

In Paper I, we calculated the average absorption in the Lyα forest region based on the ARC 3.5 m discovery spectra. Here we carry out these calculations with the Keck spectra. The results are summarized in Table 2. The table includes the measurement of the D_A and D_B parameters following Oke & Korycansky (1982), the average flux decrement in the Lyα and Lyβ forest regions, respectively, as well as the transmitted flux ratio [$\mathcal{T}(z_{\rm abs})$] defined in Paper I, measured in the highest-redshift window in each quasar that is not affected by the Lyα emission line and the proximity effect. The definitions of these quantities are given in Paper I. The transmitted flux ratio is measured in the redshift range $z_{\rm em} - 0.4 < z_{\rm abs} < z_{\rm em} - 0.2$ for all objects except SDSS 1030+0524, for which the range is $5.95 < z_{\rm abs} < 6.16$. Additional measurements of this quantity along the line of sight to each quasar at lower redshift are illustrated in Figure 2. All the measurements here and below assume an intrinsic quasar continuum $f_\nu \propto \nu^{-0.5}$ ($f_\lambda \propto \lambda^{-1.5}$), with the continuum normalized at rest-frame wavelength of 1280 ± 10 Å, a region free of major emission lines. The unknown continuum shape is a source of systematic error. However, for a wavelength window close to the Lyα emission and in the regime in which $\mathcal{T}(z_{\rm abs}) \ll 1$, this error is much smaller than the cosmic variance of $\mathcal{T}$ (see below). As in Paper I, the error bars on the D_A and D_B measurements reflect the uncertainties of the continuum shape in the Lyα forest region, while the error bars on $\mathcal{T}(z_{\rm abs})$ include only the photon noise. In calculating the average flux and the photon noise, the signal in each pixel is weighted by the inverse square of the estimated noise level in that pixel. The values in Table 2 are consistent with the measurements in Paper I, albeit with errors lower by a factor of ~ 5.

In Table 2, we also include the measurement of the redshift of the Lyman Limit System ($z_{\rm LLS}$), following the method described in Fan et al. (2000, § 4.1). Note, however, at $z \sim 6$, the flux level at the rest-frame 912 Å is so low, because of the presence of numerous Lyα forest lines from lower redshift, that this measurement is rather uncertain. The quasar spectra are consistent with no flux almost immediately blueward of rest-frame 912 Å.

Figure 2 presents the evolution of the transmitted flux ratio $\mathcal{T}$ and effective optical depth $\tau_{\rm eff}[\equiv -\ln(\mathcal{T})]$ as a function of redshift $z_{\rm abs}$. The average absorption evolves strongly with redshift. At $z_{\rm abs} \sim 3.5$, $\mathcal{T} \sim 0.4$ (e.g., Rauch et al. 1997). It decreases to $\mathcal{T} \sim 0.25$ at $z \sim 4.5$ (Songaila et al. 1999). At $z \sim 5.0$, $\langle \mathcal{T} \rangle \sim 0.12$ from Figure 2, and at $z \sim 5.5$, $\langle \mathcal{T} \rangle \sim 0.07$. The scatter of $\mathcal{T}$ at the same redshift is larger than implied by photon noise or uncertainty of the continuum shape, suggesting that the error in $\mathcal{T}$ is dominated by cosmic variance. Zuo (1993) calculated the scatter of the transmitted flux given the number density and column density distribution of Lyα clouds. Using equation (9) in that paper, we find that at $z \sim 5.5$, for $\mathcal{T} \sim 0.10$, $\sigma(\mathcal{T}) \sim 0.03$, comparable to the scatter seen in Figure 2. For $\mathcal{T} \ll 1$, $\sigma(\mathcal{T})$ is comparable to $\mathcal{T}$ itself, and it decreases rapidly toward higher redshift.

The only measurements of $\mathcal{T}$ at $z > 5.7$ come from the highest-redshift object SDSS 1030+0524. It shows that $\mathcal{T}(z_{\rm abs} = 5.75) = 0.03$. The most dramatic change in $\mathcal{T}$, however, comes from the measurement at $z \sim 6$; over the redshift range $5.95 < z_{\rm abs} < 6.16$, the average transmitted flux $\mathcal{T} = 0.0038 \pm 0.0026$. This 1.5 σ "detection" is in fact consistent with zero in our estimation; indeed, slight changes in the way we did our sky subtraction caused the value to change by of order 1 σ. Thus there is no detectable flux over the wavelength range of $8450 < \lambda < 8710$ Å, corresponding to a flux decrement of greater than 150 from the continuum level or, equivalently, to a lower limit (1 σ) on the Gunn-Peterson optical depth because of neutral hydrogen in the IGM of $\tau_{\rm GP} > 5.0$. At $\lambda > 8750$ Å, the flux is detectable again, presumably because of the effect of the ionizing photons from the luminous quasar itself (§ 4). This result confirms the measurement based on the discovery spectrum (Paper I), in which we found $\mathcal{T} = 0.003 \pm 0.020$.

TABLE 2

ABSORPTION PROPERTIES OF $z > 5.8$ QUASARS

Object	$z_{\rm em}$	$z_{\rm LLS}$	D_A	D_B	$z_{\rm abs}$	Transmitted Flux Ratio at $z_{\rm abs}$
J104433.04–012502.2	5.80	5.72	0.90 ± 0.02	0.95 ± 0.02	5.5	0.088 ± 0.004
J083643.85+005453.3	5.82	5.80	0.92 ± 0.02	0.95 ± 0.02	5.5	0.106 ± 0.001
J130608.26+035626.3	5.99	5.98	0.91 ± 0.02	0.95 ± 0.02	5.7	0.070 ± 0.003
J103027.10+052455.0	6.28	6.28	0.93 ± 0.02	0.99 ± 0.01	6.05	0.004 ± 0.003[a]

[a] The Lyβ trough gives a 1 σ lower limit to the equivalent Lyα optical depth of $\tau_{\rm eff} > 20$, which corresponds to an equivalent $\mathcal{T} < 2 \times 10^{-9}$.

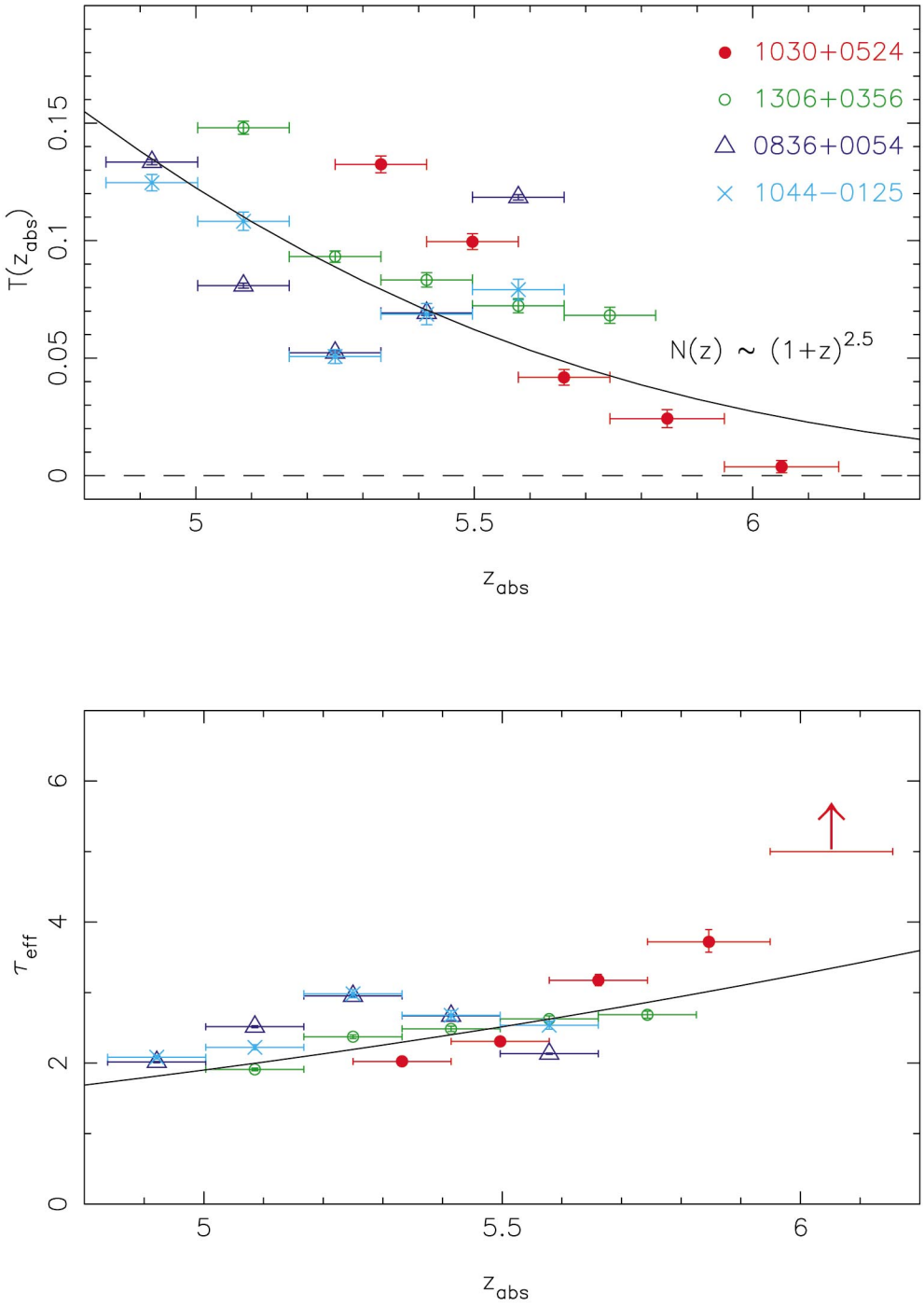

FIG. 2.—Evolution of transmitted flux ratio and effective Gunn-Peterson optical depth as functions of redshift. The solid line is the expected evolution if the number density of Lyα clouds increases as $N(z) \propto (1+z)^{2.5}$. No flux is detected in the spectrum of SDSS 1030+0524 at $z_{abs} \sim 6$, indicating $\tau_{eff} > 5.0$. The nondetection of flux in the Lyβ trough gives a substantially stronger 1 σ upper limit of $\tau_{eff} > 20$.

This is the first detection of a complete Gunn-Peterson trough, in the sense that no flux is detected over a large wavelength range in the Lyα forest region, indicating that the effective Gunn-Peterson optical depth caused by neutral hydrogen in the IGM, τ_{eff}, is much larger than 1.

Figure 3 shows the sky-subtracted two-dimensional spectrogram from the ninth order of the ESI data; note the complete absence of detected flux blueward of the Lyα emission line. Figure 3 also shows the one-dimensional spectrum and the corresponding estimated error per pixel (shaded) of SDSS 1030+0524 over the redshift range $5.75 < z < 6.25$ for both Lyα and Lyβ. As evident from the figure, the average flux level is consistent with zero for $5.95 < z < 6.16$ at both lines (8450–8710 Å for Lyα and 7130–7350 Å for Lyβ).

The effective continuum at Lyβ is affected by the Lyα forest. The effective Lyα redshift at 7240 Å, the center of the Lyβ trough, is $z \approx 5$. Figure 2 shows that at that redshift, the transmission of the Lyα forest is roughly 12%, albeit with large scatter (see also Songaila et al. 1999). Taking this

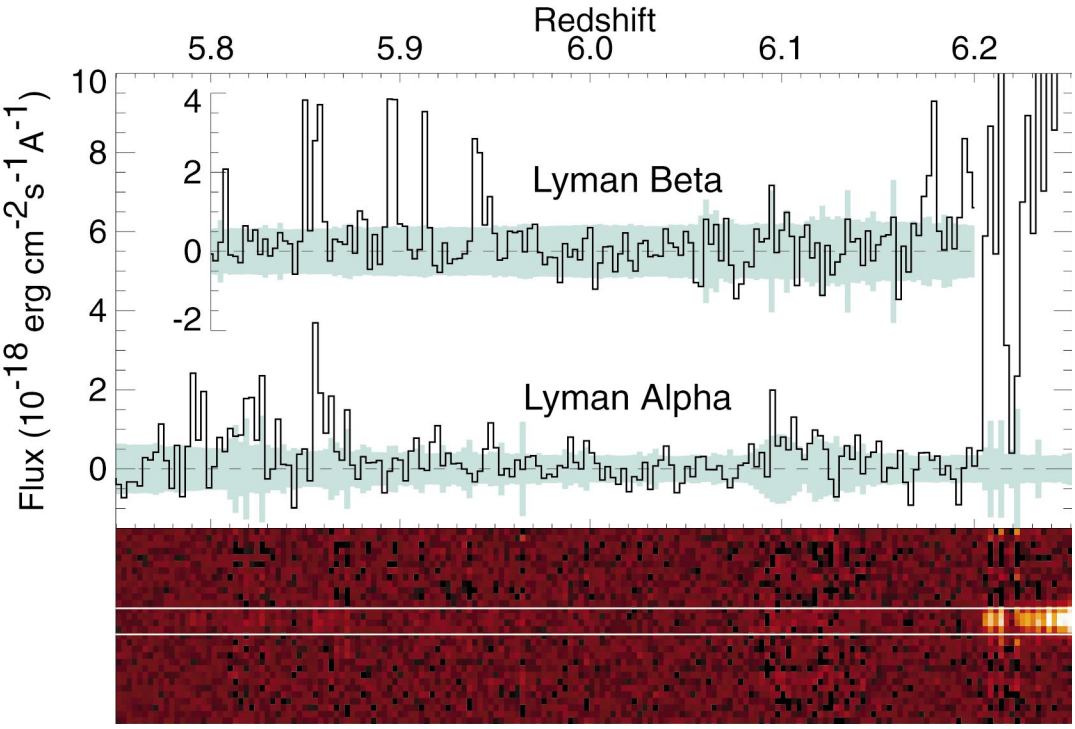

FIG. 3.—Gunn-Peterson trough in the spectrum of SDSS 1030+0524 observed with Keck/ESI. Both the Lyα and Lyβ absorption regions are shown. The bottom panel shows the sky-subtracted two-dimensional spectrum in the Lyα region. The Lyα data come from the ninth order of the echellette spectrum and cover the wavelength range 8200 to 8810 Å. The Lyβ data are the result of combining orders 7 and 8 and covering the wavelength range 6920 to 7440 Å. The green shaded areas are the 1 σ noise bands in the extracted spectra. The spectrum is very black over the redshift range $5.95 < z < 6.16$.

into account and again extrapolating the quasar continuum from redward of Lyα emission, assuming $f_\lambda \propto \lambda^{-1.5}$, gives a measured transmitted flux ratio in the Lyβ trough of -0.002 ± 0.020, a clear nondetection. The error does not include the uncertainty in the transmission of Lyα at $z = 5$, which we estimate to be approximately 20% in $\tau_{\rm eff}$ based on the scatter seen in Figure 2.

The ratio of oscillator strengths of the Lyα and Lyβ lines is 5.27 (Verner, Verner, & Ferland 1996). Thus we can convert the transmitted flux ratio in the Lyβ forest region to an *equivalent* 1 σ lower limit to the optical depth in the Lyα forest region of $\tau_{\rm eff} > 20$ (albeit with an uncertainty due to the limits of our model for the intrinsic spectrum). This limit is, in fact, considerably stronger than the limit obtained directly from the Lyα forest itself.

At $\lambda < 6980$ Å, there appears to be another break (Fig. 1); this is the start of the corresponding Lyγ Gunn-Peterson trough. We have not attempted to obtain a quantitative optical depth for this line, because of the extreme overlapping absorption from both the Lyα and Lyβ forests.

Our ability to constrain the upper limit of the flux in the Lyα and Lyβ forest regions and the corresponding lower limit to the Gunn-Peterson optical depth depend on the reliability of sky subtraction. In this case, the expression "black as night" has special significance, because, invariably, upper limits to brightness come down to the accuracy with which one can subtract the sky. Unfortunately, the night sky is not very black, especially in the near-IR region, where the sky emission is concentrated in a series of very bright OH lines that nearly blanket the spectrum. At the ESI resolution, the peak of the strongest skylines at 8000–9000 Å can be a factor of greater than 50 stronger than that of the darker region between lines. The high spectral resolution of ESI enables us to resolve the much darker regions between strong skylines and limits the number of pixels affected by the skylines. The pixels affected by strong skylines are assigned much smaller weights when we calculate the average flux and effective optical depth. It is our considered opinion that in this instance the data reduction posed no unusual difficulties and that the faint to nonexistent flux levels seen blueward of Lyα are reliable. These problems are less severe in the spectral region of the Lyβ trough, and, as we have seen, the two troughs give consistent limits on the mean optical depth.

4. DISCUSSION

The Gunn & Peterson (1965) optical depth in a uniformly distributed IGM is given by

$$\tau_{\rm GP}(z) = 1.8 \times 10^5 h^{-1} \Omega_M^{-1/2} \left(\frac{\Omega_b h^2}{0.02}\right) \times \left(\frac{1+z}{7}\right)^{3/2} \left(\frac{n_{\rm HI}}{n_{\rm H}}\right). \quad (1)$$

Only a small fraction of neutral hydrogen component in the IGM is needed to have $\tau_{\rm GP} \gg 1$ and give rise to a complete Gunn-Peterson trough. Therefore, the existence of a Gunn-Peterson trough by itself does not prove that the object is observed prior to the reionization epoch. Even if the neutral fraction were independent of redshift, one still expects the transparency of the Lyα forest to decrease with increasing redshift. In reality, the expansion of the universe and the increase in the ionizing background cause the neutral hydrogen fraction to decrease toward low redshift (see

below). The observed redshift evolution of the Gunn-Peterson optical depth in the spectrum of SDSS 1030+0524 allows us to answer an important question: Is the amount of Lyα forest absorption at $z \sim 6$ consistent with a simple extrapolation from the observations at lower redshifts? Or does it indicate a more dramatic change in the state of the IGM?

Assuming that the number density of Lyα forest lines evolves with redshift as $(1 + z)^{\gamma}$, where $\gamma \sim 2.5$ at $z \sim 4$, the effective optical depth evolves as $(1 + z)^{\gamma+1}$ (Zuo & Phinney 1993; Zuo 1993). The solid line in Figure 2 shows an extrapolation of the optical depths to higher redshifts using this simple model. It is evident that the $z \sim 6$ value from SDSS 1030+0524 deviates from this extrapolation; the observed absorption at $z \sim 6$ is stronger than that predicted by this model, assuming an ionization fraction that remains constant with redshift. A natural explanation for this difference is that the ionization fraction increases with time; i.e., the IGM was more neutral at earlier times.

Assuming that the hydrogen gas in the IGM responsible for the Lyα forest absorption is in photoionization equilibrium, wherein photoionization of the neutral hydrogen by the UV background is balanced by recombination, one can express $(n_{\rm H\,I}/n_{\rm H})$ in equation (1) in terms of the ionizing background. Doing so, the Gunn-Peterson optical depth of a uniform IGM can be expressed as (Weinberg et al. 1997),

$$\tau_{\rm GP} = 5.9 \times 10^{-4} H_0 (1+z)^6 H(z)^{-1} h^{-1} T_4^{-0.7} \times (\Omega_b h^2/0.02)^2 \Gamma_{-12}^{-1} . \quad (2)$$

Here $H(z)$ is the Hubble constant at redshift z, T_4 is the temperature of the IGM gas in units of 10^4 K, and Γ_{-12}, the photoionization rate of hydrogen in units of 10^{-12} s^{-1}, depends on the shape and amplitude of the ionizing background. Thus, in a given background cosmology, the observed evolution of the Gunn-Peterson optical depth can be used to measure the redshift evolution of the ionizing background (e.g., McDonald et al. 2000). A more accurate determination of the ionizing background should also model the gravitational evolution of the Lyα forest with redshift. Recently, McDonald & Miralda-Escudé (2001) used the transmitted flux measurement to calculate the evolution of ionizing background at $z < 5.2$. In a separate paper (Fan et al. 2001b), we use both semianalytic models and cosmological simulations to investigate the evolution of the ionizing background at higher redshifts, using the measured transmitted flux ratios and effective optical depths at $z \sim 6$.

As discussed by Miralda-Escudé (1998), the spectra of sources observed prior to complete reionization should show the red damped wing of the Gunn-Peterson trough in the red side of Lyα, because of the very large optical depth. This damped wing would, in principle, suppress the Lyα emission line. However, as shown in Madau & Rees (2000) and Cen & Haiman (2000), luminous quasars such as those discussed in this paper would ionize the surrounding regions and create H II regions of radius several megaparsecs (the "proximity" effect, Carswell et al. 1982). The presence of these quasar H II regions results in a much higher transmission redward of Lyα; thus the emission-line profile is less affected by the red damped wing (see also Fan et al. 2001b). Therefore, the presence of the Lyα emission line and the absence of the red damped wing are not by themselves indicators that the IGM was already ionized at this redshift. The true extent of the proximity effect in SDSS 1030+0524 is probably best defined by the transmission of Lyβ emission at a redshift of 6.18 (see Fig. 3).

The size of the H II region associated with the quasar depends on the luminosity and lifetime of the quasar and the clumpiness of the IGM. In principle, we could use the proximity effect to constrain the amplitude of the ionizing background (Bajtlik, Duncan, & Ostriker 1988) by determining the distance from the quasar at which the optical depth of the Lyα forest is half that in the Gunn-Peterson trough. However, we only have a lower limit on the latter, and so at best we can only put a lower limit on the distance, and thus an upper limit on the ionizing background. We have calculated this upper limit and find that it gives a much weaker constraint than comparing the data with detailed simulations (Fan et al. 2001b). Further, clumpiness of the gas distribution near the quasar on these length scales will also increase the absorption blueward of Lyα and hence lead to an artifically higher estimate of the ionizing background.

Could any local effect produce the apparent Gunn-Peterson trough in the spectrum of SDSS 1030+0524? A 300 Å region at $z \sim 6$ corresponds to a comoving distance of $\sim 70\ h^{-1}$ Mpc ($\Omega = 0.3$, $\Lambda = 0.7$), much larger than any large-scale structure at that redshift. It is also unlikely to be a very strong damped Lyα absorption system, as we do not see any corresponding metal lines (such as Si IV λ1402). We are not aware of any known damped Lyα absorption line at lower redshifts with an EW of $\sim$300 Å. At $z_{\rm abs} \sim 6.05$, it would have a rest frame EW of $\sim$42 Å, and $N_{\rm H\,I} \sim 10^{21.5}$ cm^{-2}. Using the statistics of Storrie-Lombardi, Irwin, & McMahon (1996), we expect to find only 0.02 such systems per unit redshift at $z \sim 6$. Moreover, one would expect to see associated metal lines from such a strong absorber, which are clearly not present.

However, we emphasize that the complete Gunn-Peterson trough is observed in only one (the highest-redshift) object, and if the reionization is nonuniform, one may not see exactly the same dependence of the Gunn-Peterson trough with redshift along other lines of sight. In order to gain a more complete understanding of the IGM at $z \gtrsim 6$, more lines of sight are clearly needed. The SDSS is expected to find $\sim$20 quasars at $z \gtrsim 6$ over the course of the survey (Paper I), so we can look forward to opportunities to study this question in detail over the next few years.

The Sloan Digital Sky Survey (SDSS) is a joint project of the University of Chicago, Fermilab, the Institute for Advanced Study, the Japan Participation Group, Johns Hopkins University, the Max Planck Institute for Astronomy, the Max Planck Institute for Astrophysics, New Mexico State University, Princeton University, the United States Naval Observatory, and the University of Washington. Apache Point Observatory, site of the SDSS telescopes, is operated by the Astrophysical Research Consortium. Funding for the project has been provided by the Alfred P. Sloan Foundation, the SDSS member institutions, the National Aeronautics and Space Administration, the National Science Foundation, the Department of Energy, the Japanese Monbukagakusho, and the Max Planck Society. The SDSS Web site is http://www.sdss.org. We acknowledge support from NSF grants AST 98-02791 and AST 98-02732 and the Institute of Geophysics and Planetary Physics (operated under the auspices of the Department

of Energy by Lawrence Livermore National Laboratory under contract W-7405-Eng-48) (R. H. B.), from NSF grant PHY00-70928 and a Frank and Peggy Taplin Fellowship (X. F.), from the Space Telescope Science Institute (R. L. W.), and from NSF grant AST 00-71091 (M. A. S.). We wish to thank an anonymous referee for correcting an error in the interpretation of the Lyβ absorption. Thanks to David Helfand for his support during the Keck observing run and for cooking R. H. B. and R. L. W. a fine dinner while we were observing.

REFERENCES

Bajtlik, S., Duncan, R. C., & Ostriker, J. P. 1988, ApJ, 327, 570
Carswell, R. F., Whelan, J. A. J., Smith, M. G., Boksenberg, A., & Tytler, D. 1982, MNRAS, 198, 91
Cen, R., & Haiman, Z. 2000, ApJ, 542, L75
Dessauges-Zavadsky, M., D'Odorico, S., McMahon, R. G., Molaro, P., Ledoux, C., Péroux, C., & Storrie-Lombardi, L. J. 2001, A&A, 370, 426
Djorgovski, S. G., Castro, S. M., Stern, D., & Mahabal, A. A. 2001, ApJ, submitted
Epps, H. W., & Miller, J. S. 1998, Proc. SPIE, 3355, 48
Fan, X., et al. 2000, AJ, 120, 1167
——. 2001a, AJ, in press (Paper I)
——. 2001b, in preparation
Goodrich, R., et al. 2001, ApJ, submitted
Gunn, J. E., & Peterson, B. A. 1965, ApJ, 142, 1633
Hamann, F., & Ferland, G. 1993, ApJ, 418, 11
Krolik, J., & Voit, M. 1998, ApJ, 497, L5
Madau, P., & Rees, M. J. 2000, ApJ, 542, L69
Massey, P. 1988, ApJ, 328, 315
Massey, P., & Gronwall, C. 1990, ApJ, 358, 344
McDonald, P., & Miralda-Escudé, J. 2001, ApJ, 549, L11
McDonald, P., Miralda-Escudé, J., Rauch, M., Sargent, W. L. W., Barlow, T. A., Cen, R., & Ostriker, J. P. 2000, ApJ, 543, 1
Miralda-Escudé, J. 1998, ApJ, 501, 15
Oke, J. B., & Korycansky, D. G. 1982, ApJ, 255, 11
Péroux, C., Storrie-Lombardi, L. J., McMahon, R. G., Irwin, M., & Hook, I. M. 2001, AJ, 121, 1799
Rauch, M., et al. 1997, ApJ, 489, 7
Scheuer, P. A. G. 1965, Nature, 207, 963
Schneider, D. P, Schmidt, M., & Gunn, J. E. 1991, AJ, 101, 2004
Shklovsky, I. S. 1964, Astron. Zh., 41, 408
Songaila, A., Hu, E. M., Cowie, L. L., & McMahon, R. G. 1999, ApJ, 525, L5
Storrie-Lombardi, L., Irwin, M., & McMahon, R. 1996, MNRAS, 282, 1330
Verner, D. A., Verner, E. M. & Ferland, G. J. 1996, Atomic Data Nuclear Data Tables (San Diego: Acad. Press), 64, 1
Weinberg, D. H., Miralda-Escudé, J., Hernquist, L., & Katz, N. 1997, ApJ, 490, 564
York, D. G., et al. 2000, AJ, 120, 1579
Zuo, L. 1993, A&A, 278, 343
Zuo, L., & Phinney, E. S. 1993, ApJ, 418, 28